Available online at www.sciencedirect.com
SCIENCE DIRECT®
Journal of Organometallic Chemistry 689 (2004) 317–325
Journal of Organometallic Chemistry
www.elsevier.com/locate/jorganchem

Synthesis and spectroscopic studies of diorganotin derivatives with 2-[(2,6-dimethylphenyl)amino]benzoic acid. Crystal and molecular structure of the first complexes of 2-[(2,6-dimethylphenyl)amino]benzoic acid. Crystal and molecular structures of 1,2:3,4-di-μ_2-2-[(2,6-dimethylphenyl)amino]-benzoato-*O,O*-1,3-bis-2-[(2,6-dimethylphenyl)amino]benzoato-*O*-1,2,4:2,3,4-di-μ_3-oxo-tetrakis[di-butyltin(IV)] and bis-2-[(2,6-dimethylphenyl)amino]benzoato-di-*n*-butyltin(IV)

Vaso Dokorou [a], Mavroudis A. Demertzis [a], Jerry P. Jasinski [b], Dimitra Kovala-Demertzi [a,*]

[a] *Inorganic Chemistry, Department of Chemistry, University of Ioannina, 45110 Ioannina, Greece*
[b] *Department of Chemistry, Keene State College, 229 Main Street, Keene, NH 03435-2110, USA*

Received 16 September 2003; accepted 16 October 2003

Abstract

The complexes $[Bu_2(DMPA)SnOSn(DMPA)Bu_2]_2$ (**2**) and $[Bu_2Sn(DMPA)_2]$ (**3**), where HDMPA is 2-[bis(2,6-dimethylphenyl)amino]benzoic acid, have been prepared and structurally characterized by means of, vibrational, ultra-violet, ^1H and ^{13}C NMR spectroscopies. The crystal structure of complexes **2** and **3** have been determined by X-ray crystallography. Three distannoxane rings are present to the dimeric tetraorganodistannoxane of planar ladder arrangement of **2**. The structure is centro-symmetric and features a central rhombus Sn_2O_2 unit with two additional tin atoms linked at the O atoms. Five- and six-coordinated tin centers are present in the dimmer distannoxane. The crystal structure of **3** consists of discrete molecular units and the two modeprononated ligands are co-ordinated to the $SnBu_2$ fragment. The ligands act as anisobidentate chelating agents, thus rendering the tin atom six-co-ordinated. Significant $\pi \rightarrow \pi$, C–H-π stacking interactions and intramolecular hydrogen bonds stabilize the structures **2** and **3**. The polar imino hydrogen atom participates in intramolecular hydrogen bonds. Complexes **2** and **3** are self-assembled via $\pi \rightarrow \pi$ C–H-π and stacking interactions.

Keywords: 2-[bis(2,6-dimethylphenyl)amino]benzoic acid; Diorganotin adducts; Crystal structures; Spectroscopic studies

1. Introduction

2-[(2,6-dimethylphenyl)amino]benzoic acid or *N*-(2,6-dimethylphenyl)anthranilic acid), HDMPA, 1, Scheme 1, resembles mefenamic, tolfenamic, flufenamic acids and other fenamates in clinical use. HDMPA was found to inhibit by 48.0% on triiodothyronine (T_3) uptake by H4 hepatocytes and octanol–water partition coefficient was found to be 5.337 [1a]. The anti-inflammatory activity of HDMPA's was measured by the anti-UV-erythema test and the minimum effective dose (MED) was found to be 50 mg/kg [1b].

Organotin(IV) carboxylates form an important class of compounds and have been receiving increasing attention in recent years, not only because of their intrinsic interest but owing to their varied applications. Some

* Corresponding author. Tel.: +30-265098425; fax: +30-265044825.
E-mail address: dkovala@cc.uoi.gr (D. Kovala-Demertzi).

0022-328X/$ - see front matter © 2003 Elsevier B.V. All rights reserved.
doi:10.1016/j.jorganchem.2003.10.018

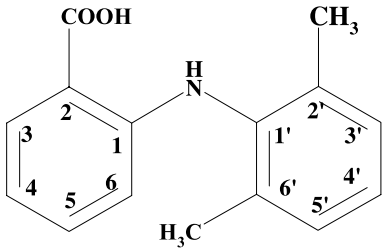

Scheme 1.

examples find wide use as catalysts and stabilizers, and certain derivatives are used as biocides, as anti-fouling agents and as wood preservatives [2]. Information on the structures of organotin carboxylates continues to accumulate, and at the same time new applications of such compounds are being discovered in industry, ecology and medicine. In recent years, investigations have been carried out to test their anti-tumour activity and it has been observed that indeed several diorganotin species, as well as triorganotin species, show potential as anti-neoplastic agents [3].

It was thought of interest to explore the chemistry of organotin/phenylanthranilic acid compounds, as a continuation of our studies of organotin chemistry [4] and on the coordination chemistry of non-steroidal anti-inflammatory drugs, phenylanthranilic acids such as diclofenac, mefenamic and tolfenamic acids [5]. The novel complexes $[Bu_2(DMPA)SnOSn(DMPA)Bu_2]_2$(**2**) and $[Bu_2Sn(DMPA)_2]$ (**3**) (DMPA is the deprotonated *N*-(2,6-dimethylphenyl)anthranilic acid), have been structurally characterized by means of vibrational, ultraviolet and ^{1}H- and ^{13}C-NMR spectroscopic studies, and the crystal and molecular structures of **2** and **3** are described.

2. Experimental details

2.1. General and instrumental

The reagents (Aldrich, Merck) were used as supplied while the solvents were purified according to standard procedures. Melting points were determined in open capillaries and are uncorrected. Infrared and far-infrared spectra were recorded on a Nicolet 55XC Fourier transform spectrophotometer using KBr pellets (4000–400 cm^{-1}) and nujol mulls dispersed between polyethylene disks (400–40 cm^{-1}). UV spectra were acquired with a JASCO V-570 spectrophotometer UV/VIS/NIR. The ^{1}H (250.13 MHz), ^{13}C (62.90 MHz) NMR spectra were recorded on a Bruker AMX-400 and on a Bruker AC-250 spectrometer. Samples were dissolved in $CDCl_3$ and spectra were obtained at room temperature with the signal of free $CDCl_3$ (at 7.24 ppm) as a reference.

2.2. Synthesis

HDMPA (1). HDMPA was synthesized according to published procedure, the Ullmann–Goldberg condensation [1]. 2,6-dimethylbenzenamine (5.60 g, 46 mmol), potassium 2-bromobenzoate (11.36 g, 47 mmol), 4-ethylmorpholine (5.46 g, 47 mmol) and 0.5 g of anhydrous copper acetate in 20 ml of distilled *N*,*N*-dimethylformamide under nitrogen atmosphere were refluxed at 145° for 3 h. In the resulting solution was added 13 ml of distilled *N*,*N*-dimethylformamide, and 19 ml of 12% hydrochloric acid. The aqueous layer was decanted and methanol was added. The solid was collected and recrystallized three times from acetone., m.p.: 209–210°; Yield 24,35% (2,70 gr). Anal. Found: C, 73.94; H, 6.59; N, 5.79. Calc.: C, 74.18; H, 6.46; N, 5.81%.

$[Bu_2(DMPA)SnOSn(DMPA)Bu_2]_2$ (2). Di-*n*-butyl oxide (0.286 g, 1.15 mmol), HDMPA (0.2410 g, 1.0 mmol) and 40 ml of benzene were refluxed overnight with azeotropic removal of water via a Dean–Stark trap. The resulting clear solution was rotary evaporated under vacuum to a small volume (3 ml), chilled and triturated with acetone to give a white solid. The white powder was dried in vacuo over silica gel. m.p. 160–162 °C; yield 35%. Anal. Found: C, 57.30; H, 6.83; N, 2.76. Calc.: C, 57.41; H, 6.70; N, 2.91%.

Crystals of **2** suitable for X-ray analysis were obtained by slow evaporation of a fresh $CHCl_3$/EtOH solution.

$[Bu_2Sn(DMPA)_2]$ (3). Di-*n*-butyltin(IV) oxide (0.2489 g, 1 mmol), HDMPA (0.5187 g, 2.15 mmol), and 40 ml of benzene were refluxed for 24 h with azeotropic removal of water via a Dean–Stark trap. The resulting clear solution was rotary evaporated under vacuum to a small volume. Drops of acetone were added and, after slow evaporation, white powder was isolated, m.p. 115–117 °C; yield 78.30%. Anal. Found: C, 64.10; H, 6.70; N, 3.97. Calc.: C, 63.98; H, 6.49; N, 3.93%.

Crystals of **3** suitable for X-ray analysis were obtained by slow evaporation of a fresh C_6H_6/CH_3CN solution.

2.3. X-ray crystallography

Crystal data are given in Table 1, together with refinement details. All measurements of crystals were performed on a Rigaku AFC6S diffractometer with graphite monochromated Mo Kα radiation. The data were collected using the ω–2θ scan technique to a maximum 2θ value of 55.0°. Omega scans of several intense reflections, made prior to data collection, had an average width at half-height of 0.31° and 0.23° for **2** and **3** respectively with a take-off angle of 6.0°. Scans of $(1.52 + 0.34 \tan\theta)°$ were made at a speed of 8.0°/min (in ω). The weak reflections ($I < 10.0\sigma(I)$) were rescanned (maximum of four scans) and the counts were accumulated to ensure good counting statistics. Stationary

Table 1
Crystal data and refinement for **2** and **3**

	2	**3**
Empirical formula	$C_{92}H_{128}N_4O_{10}Sn_4$	$C_{38}H_{46}N_2O_4Sn$
Formula weight	1924.82	713.48
Temperature/K	296	296
Wavelength/Å	Mo Kα 0.71069	Mo Kα 0.71069
Crystal system	Triclinic	Triclinic
Space group	*P*-1	*P*-1
a/Å	12.275(4)	12.234(4)
b/Å	19.340(6)	16.148(5)
c/Å	11.438(4)	10.449(4)
α/°C	90.89(3)	98.50(3)
β/°C	116.11(3)	114.90(3)
γ/°C	71.97(3)	71.01(3)
Volume/Å^3	2295.3(16)	1770.3(12)
Z	1	2
D_c/mg m^{-3}	1.335	1.339
Absorption coefficient, μ/mm^{-1}	1.132	0.762
F(0 0 0)	988	740
Crystal size/mm	0.30 × 0.40 × 0.50	0.20 × 0.40 × 0.50
Diffractometer	Rigaku AFC6S	Rigaku AFC6S
θ range for data collection/°C	1.9, 27.5	1.9, 27.5
Ranges of *h*, *k*, *l*	0: 15; −23: 25; −14: 13	0: 15; −19: 20; −13: 12
Reflections collected	11027	8499
Independent reflections (R_{int})	10532 (0.095)	8115 (0.136)
Data/parameters	10532/496	8115/406
Goodness-of-fit (F^2)	1.08	0.98
Final R_1/wR_2 indices ($I > 2\sigma_I$)	0.0524, 0.2099	0.0563, 0.2027
Largest difference peak/hole/e Å^{-3}	1.65/−1.86	−0.86, 0.69

background counts were recorded on each side of the reflection. The ratio of peak counting time to background counting time was 2:1. The diameter of the incident beam collimator was 1.0 mm, the crystal to detector distance was 400 mm, and the detector aperture was 9.0 × 13.0 mm (horizontal × vertical). The structure **2** was solved by heavy-atom Patterson methods [6a] and **3** by direct methods [6b] and expanded using Fourier techniques [6c]. The structures were refined by the full-matrix least-squares method on all F^2 data using the SHELXL97 programs [6d]. The non-hydrogen atoms were refined anisotropically. Hydrogen atoms were located by difference maps and refined isotropically. Neutral atom scattering factors were taken from Cromer and Waber [7a]. Anomalous dispersion effects were included in Fcalc [7b]; the values for $\Delta f'$ and $\Delta f''$ were those of Creagh and McAuley [7c]. All calculations were performed using the teXsan [7d] crystallographic software package of Molecular Structure Corporation except for refinement, which was performed using SHELXL-97 [6d].

3. Results and discussion

3.1. Crystal structures of **2** and **3**

Compounds **2** and **3** are obtained by azeotropic removal of water from the reaction between the di-*n*-butyl oxide and HDMPA acid in the molar ratio 1:1 and 1:2 respectively conducted in benzene. The molecular

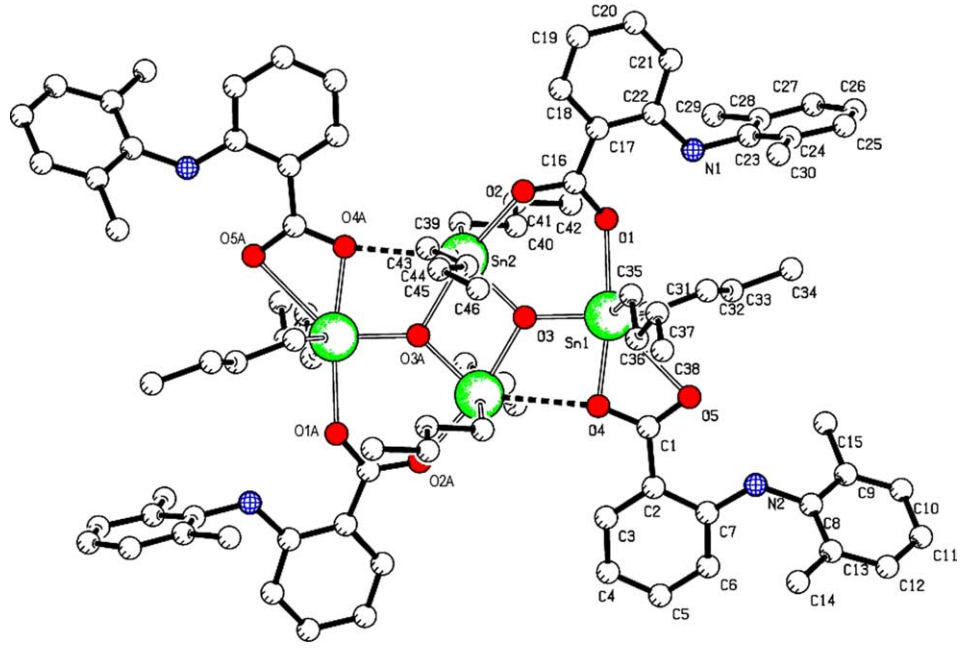

Fig. 1. Perspective view of $[Bu_2(DMPA)SnOSn(DMPA)Bu_2]_2$ (**2**) showing the atomic numbering scheme.

Table 2
Bond lengths (Å) and angles (°) for **2** and **3**

2		**3**	
Sn(1)–O(1)	2.325(9)	Sn(1)–O(2A)	2.085(6)
Sn(1)–O(3)	2.021(6)	Sn(1)–O(2B)	2.064(6)
Sn(1)–O(4)	2.172(8)	Sn(1)–O(1A)	2.562(7)
Sn(1)–C(31)	2.118(11)	Sn(1)–O(1B)	2.563(7)
Sn(1)–C(35)	2.115(14)	Sn(1)–C(16A)	2.106(10)
Sn(2)–O(2)	2.241(9)	Sn(1)–C(16B)	2.112(11)
Sn(2)–O(3)	2.041(6)	O(1A)–C(1A)	1.246(11)
Sn(2)–C(39)	2.118(9)	O(1B)–C(1B)	1.234(10)
Sn(2)–C(43)	2.123(11)	O(2A)–C(1A)	1.298(12)
Sn(2)–O(3)[a]	2.193(7)	O(2B)–C(1B)	1.285(11)
O(1)–C(16)	1.271(14)	N(1A)–C(3A)	1.367(11)
O(2)–C(16)	1.250(12)	N(1A)–C(8A)	1.412(12)
O(4)–C(1)	1.296(12)	N(1B)–C(3B)	1.358(10)
O(5)–C(1)	1.238(13)	N(1B)–C(8B)	1.441(11)
N(1)–C(22)	1.396(15)		
N(1)–C(23)	1.418(14)		
N(2)–C(7)	1.382(14)		
N(2)–C(8)	1.419(14)		
O(1)–Sn(1)–O(3)	89.0(3)		
O(1)–Sn(1)–O(4)	170.0(2)	O(2A)–Sn(1)–O(2B)	83.1(2)
O(1)–Sn(1)–C(31)	83.6(4)	O(2A)–Sn(1)–C(16A)	103.7(4)
O(1)–Sn(1)–C(35)	82.8(4)	O(2A)–Sn(1)–C(16B)	109.3(3)
O(3)–Sn(1)–O(4)	82.1(2)	O(2B)–Sn(1)–C(16A)	111.2(3)
O(3)–Sn(1)–C(31)	111.6(4)	O(2B)–Sn(1)–C(16B)	102.5(4)
O(3)–Sn(1)–C(35)	109.4(4)	C(16A)–Sn(1)–C(16B)	134.9(4)
O(4)–Sn(1)–C(31)	95.4(4)	O(1A)–Sn–O(1B)	168.0(2)
O(4)–Sn(1)–C(35)	104.4(4)	O(2B)–Sn–O(2A)	83.1(2)
C(31)–Sn(1)–C(35)	136.4(5)	O(2B)–Sn–O(1B)	54.5(2)
O(2)–Sn(2)–O(3)	91.7(3)	O(2A)–Sn–O(1A)	55.1(2)
O(2)–Sn(2)–C(39)	91.5(4)	O(2A)–Sn–O(1B)	136.8(2)
O(2)–Sn(2)–C(43)	84.5(4)		
O(2)–Sn(2)–O(3)][a]	167.2(3)		
O(3)–Sn(2)–C(39)	108.9(4)		
O(3)–Sn(2)–C(43)	109.6(4)		
O(3)–Sn(2)–O(3)[a]	76.6(2)		
C(39)–Sn(2)–C(43)	141.5(5)		
O(3)[a]–Sn(2)–C(39)	97.1(4)		
O(3)[a]–Sn(2)–C(43)	94.6(4)		
Sn(1)–O(1)–C(16)	131.0(6)		
Sn(2)–O(2)–C(16)	134.7(8)		
Sn(1)–O(3)–Sn(2)	134.6(3)		
Sn(1)–O(3)–Sn(2)[a]	121.6(3)		
Sn(2)–O(3)–Sn(2)[a]	103.4(2)		
Sn(1)–O(4)–C(1)	106.0(6)		

[a] Symmetry operation (i) $-x$, $1-y$, $1-z$.

structure of **2** is shown in Fig. 1 and selected interatomic parameters are collected in Table 2.

Compound **2** is a centrosymmetric dimmer distannoxane built up around the planar cyclic Sn_2O_2 unit. The two oxygen atoms of this unit are tridentate as they link three Sn centres, two endo-cyclic and one exo-cyclic. The distance between the endocyclic and exocyclic tin atoms is 3.7483(16) and the distance between the two endocyclic tin centers is 3.3240(16). The additional links between the endo- and exo-cyclic Sn atoms are provided by bidentate carboxylate ligands that form asymmetrical bridges (Sn(1)–O(1) 2.325(9) Å and Sn(2)–O(2) 2.241(4) Å). Each exocyclic Sn atom is also coordinated by an anisobidentate chelating carboxylate ligand (Sn(1)–O(4) 2.172(8) Å and Sn(1)–O(5) 2.736(9) Å). The Sn(1)–O(5) distance 2.736(9) Å is considered long to indicate significant bonding interactions, however, the range of distances Sn–O of 2.61–3.02 Å, has been confidently reported for intramolecular bonds [8].

Analysis of the shape determining angles for **2**, using the approach of Reedijk and coworkers [9], yields $\tau((\alpha-\beta)/60)$ a value of 0.43 for Sn(2) ($\tau = 0.0$ and 1.0 for *SP* and *TBP* geometries respectively). The metal coordination geometry is therefore described as distorted square pyramidal with the O(3) atom occupying the apical positions for Sn(2). The donor O(3) is chosen as apex by the simple criterion that it should not be one of the oxygens which define either of the two largest

L–Sn–L angles, α and β [9]. Distortions from the ideal geometries may be related to the close approach 2.918(6) Å of the O(4A) atom to Sn(2), (symmetry operation *i*: $-x, 1-y, 1-z$). This distance is long for primary Sn–O bonding, but represent a type of secondary interaction [5]. The structures of dimeric distannoxane of anthranilic acid, $[Me_2(NH_2\text{-}o\text{-}H_4C_6CO_2)SnOSn(NH_2\text{-}o\text{-}H_4C_6CO_2)Me_2]_2$ and its *p*-isomer$[Me_2(NH_2\text{-}po\text{-}H_4C_6CO_2)SnOSn(NH_2\text{-}p\text{-}H_4C_6CO_2)Me_2]_2$ were reported by Holmes et al. [10]. The *o*-isomer has solid state structure closely resembling the **2**, both in the geometry of the central core $(Sn_2O_2)_2$, the coordination mode of anthranilic acid and the presence of weaker interactions (2.746(7)–2.909(6)), while the *p*-isomer exhibits all anisobidentate chelating carboxylate ligands [10]. For **2**, the Sn(1)–O(1), Sn(2)–O(2) bond distances involving the bridging carboxylate ligand, 2.325(9) and 2.241(9) Å respectively, differ by only 0.084 Å indicating a nearly symmetrical bridge. The anisobidentate bidentate carboxylate has a difference of 0.058 Å between its C–O bonds while for the bidentate carboxylato this difference is only 0.021 Å; the variations in the C–O bond distances suggest charge delocalization over the carboxylato group COO. The different modes of bonding of the acetates, i.e. bridging or chelating, are thus easily differentiated by the relevant bond lengths.

The phenyl rings are planar. The dihedral angles between the planes of the phenyl rings for **2** are 81.7(9) and 59.6(6)° for the bidentate bridging and the anisobidentae chelating ligands respectively. The aminobenzoate portion of each carboxylato ligand is effectively planar which presumably facilitates the formation of intramolecular N(1)–H···O(1) and N(2)–H···O(5) interactions of 2.654(13) and 2.662(14) Å, respectively. The crystal structure of **2** shows ring stacking interactions. The monomers are stacked to a chain by double strong $\pi \rightarrow \pi$ interactions (C(2)–C(7) → C(17)–C(22), C(17)–C(22) → C(2)–C(7); the phenyl rings C(2)–C(7) and C(17)–C(22) 'face' the phenyl rings C(17)–C(22) and C(2)–C(7) respectively at a distance of 3.941 Å). These $\pi \rightarrow \pi$ interactions play an important role in the stabilization of the stacked molecular chains. In addition, C–H → π play a role in the stabilization of the chains. The butyl groups are pointed between the layers into the channels. In this case complex **2** is self-assembled via C–H-π and $\pi \rightarrow \pi$ stacking interactions. View of the crystal packing along the *b* axis for **2** is shown in Fig. 2. The polar imino hydrogen atoms on N(1), and N(2) participate in a bifurcated intramolecular hydrogen bond system, as shown in Table 3. The overall geometry found in **2**, allowing for differences in chemistry, is remarkably similar to compounds with the general formula $[R_2(R'CO_2)SnOSn(O_2CR')R_2]_2$ [11].

The molecular structure of **3** is shown in Fig. 3 and selected interatomic parameters are collected in Table 2.

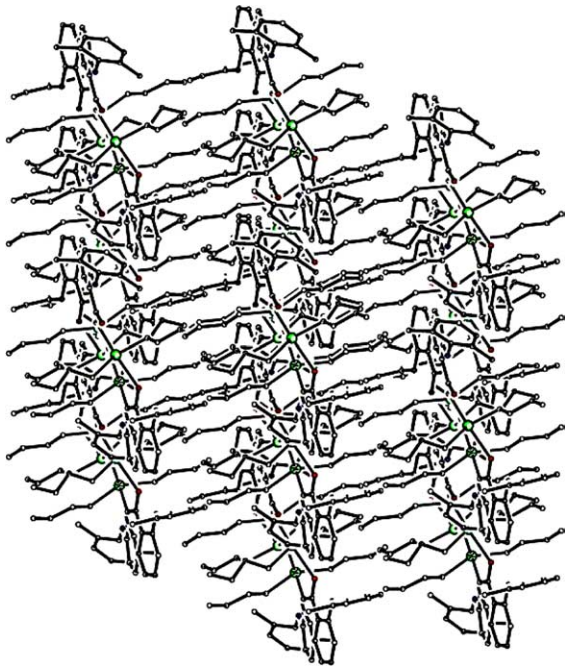

Fig. 2. Packing diagram of $[Bu_2(DMPA)SnOSn(DMPA)Bu_2]_2$ (**2**) viewed along the *b* axis.

The complex **3** comprise discrete molecular units, in which the carboxylato group functions as an anisobidentate chelating ligand [Sn–O(2A) 2.085(6), Sn–O(1A) 2.562(7) and Sn–O(2B) 2.064(6), Sn–O(1A) 2.563(7) respectively for the two ligands], thus rendering the tin atom six-coordinated. The intramolecular hydrogen bond formed from the imino group N(1A) and N(1B) contributes in causing the longer Sn–O(1a) and Sn–O(1B) bonds. The two C–O bond distances of the carbonyl group are unequal [0.049 and 0.052 are the bond differences for the two ligands Å] with the longer C–O distance being associated with the shorter Sn–O bond and vice versa. The phenyl rings are planar. The dihedral angle between the planes of the phenyl rings in **3** is 86.7(5) and 75.4(4) for the two ligands C(1A)–C(15A) and C(1B)–C(15B) respectively. The crystal structure of **3** shows C–H-π interactions and intramolecular hydrogen bonds. The polar imino hydrogen atoms on N, participates in an intramolecular hydrogen bond, Table 3. Complex **3** is self-assembled via C–H-π and $\pi \rightarrow \pi$ stacking interactions.

3.2. Spectroscopy

3.2.1. Infrared spectroscopy

The most prominent absorptions are shown in Table 4. As the carboxylic hydrogen is more acidic than the imino hydrogen the deprotonation occurs in the carboxylic group. This is confirmed by the IR spectra of the complexes, showing the characteristic bands for the secondary amino groups and for the coordinated carboxylate group [12]. The strong band at 3340 cm^{-1},

Table 3
Distances (Å) and angles (°) of C–H-π, π → π interactions and intramolecular hydrogen bonds for **2** and **3**

C–H-π, π–π interactions and intramolecular hydrogen bonds for **2**					
C–H(I) → Cg(J)			H–Cg	C–Cg	∠C–H–Cg
C(15)–H(5) → Cg(4)[i]			2.9607	3.741(19)	141.13
C(30)–H(23) → Cg(4)[ii]			3.0084	3.85(2)	153.86
Cg(I) → Cg(J)[a]		Cg–Cg[b]	β[c]	CgI-Perp[d]	CgJ-Perp[e]
Cg(3) → Cg(5)[iii]		3.941(7)	16.18	3.568	3.784
Cg(5) → Cg(3)[ii]		3.941(7)	25.10	3.785	3.568
D	H	A	D···A	H···A	∠D–H···A
N(1)	H(63)	O(1)	2.654(13)	1.91	130
N(2)	H(64)	O(5)	2.662(14)	1.92	130
C(15)	H(4)	N(2)	2.846(17)	2.43	106
C(14)	H(15)	N(2)	2.949(18)	2.61	101
C(30)	H(24)	N(1)	2.859(19)	2.36	111
C–H-π, π–π interactions and intramolecular hydrogen bonds for **3**					
C–H(I) → Cg(J)			H–Cg	C–Cg	∠C–H–Cg
C(12B)–H(8) → Cg(3)[iv]			3.152	3.935(13)	140.52
C(19B)–H(27) → Cg(4)[iv]			3.2304	3.95(2)	134.09
C(19A)–H(31) → Cg(2)[vi]			3.2978	3.69(3)	107.92
C(19A)–H(32) → Cg(2)[vi]			3.2379	3.69(3)	110.39
		Cg–Cg[b]	β[c]	CgI-Perp[d]	CgJ-Perp[e]
Cg(3) → Cg(3)[vii]		3.745(6)	17.03	3.581	
D	H	A	D···A	H···A	∠D–H···A
N(1A)	H(45)	O(1A)	2.701(11)	2.04	124
N(1B)	H(46)	O(1B)	2.665(10)	1.99	124
C(7B)	H(12)	O(2B)	2.734(12)	2.40	100
C(14A)	H(1)	N(1A)	2.842(14)	2.43	106
C(15A)	H(20)	N(1A)	2.842(15)	2.38	109
C(15B)	H(21)	N(1B)	2.874(16)	2.41	110
C(14B)	H(24)	N(1B)	2.868(13)	2.38	111

[a] Where Cg(1), Cg(4), Cg(3) and Cg(5), are referred to the centroids Sn(2)–O(3)–Sn(2a)–O(3a), C(9)–C(12), C(2)–C(7) and C(17)–C(22) for **2**, Cg(2), Cg(3) and Cg(4), are referred to the centroids C(2b)–C(7b), C(8a)–C(13a), C(8b)–C(13b) for **3**.

[b] Cg–Cg is the distance between ring centroids; symmetry transformations, (i) $-x, -y, 1-z$; (ii) $-1+x, y, z$; (iii) $-1+x, y, z$; (iv) $1+x, y, -1+z$; (v) $2-x, 1-y, 1-z$; (vi) $2-x, -y, 1-z$; (vii) $1-x, 1-y, 2-z$.

[c] Where β is the angle Cg(I)→Cg(J) or Cg(i)→Me vector and normal to plane I (°).

[d] CgI-Perp is the perpendicular distance of Cg(I) on ring J.

[e] CgJ-Perp is the perpendicular distance of Cg(J) on ring I.

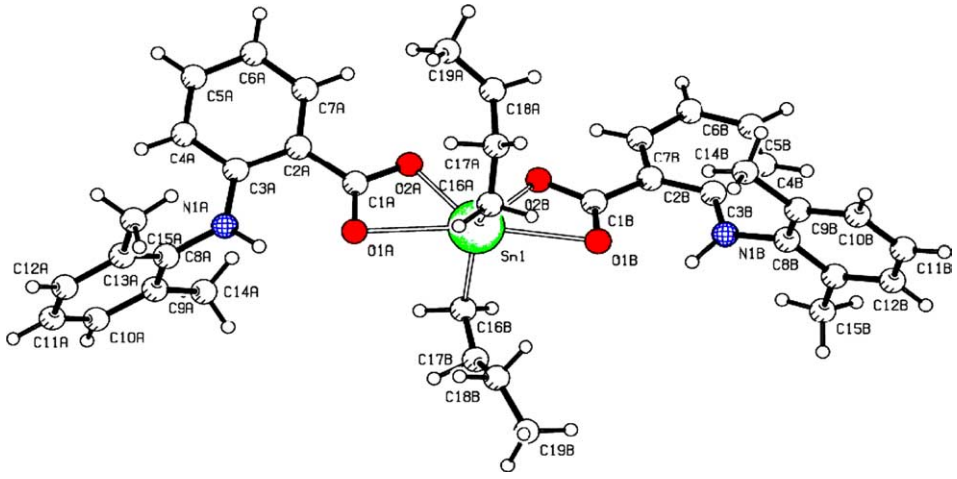

Fig. 3. Perspective view of $[Bu_2Sn(DMPA)_2]$ (**3**) showing the atomic numbering scheme.

Table 4
Selected IR (cm^{-1}) of organotin(IV) complexes

No	ν(NH)	ν_{as}(COO)	ν_{sym}(COO)	Δ	$\nu(SnO)_2$	ν(SnC)	ν(SnO)	δ(SnO)
NaDMPA	3348s 3289s 2980br	1610s	1448s	162				
2	3319s 3258s	1615s 1576s	1388s 1452s	227 124	481s 426s	529ms 506ms	295s 245m	172m 147m
3	3314s	1618s	1368	250		519ms 503m	291ms 251m	180m 149m

which appears in the IR spectra of the ligand, is assigned to the NH stretching motion and the broad band at 2980 cm^{-1} is taken to represent the ν(NH···O) mode, due to intramolecular hydrogen bonding [4,5,12]. The absence of large systematic shifts of the ν(NH) and δ(NH) bands in the spectra of the complexes compared with those of the ligand indicates that there is no interaction between the NH group and the metal ions, which is also confirmed by X-ray analysis. The ν_{as}(COO) and ν_{sym}(COO) bands appear at ~1610–1500 and ~1450–1260 cm^{-1}, respectively [12]. The difference, $\Delta[\nu_{as}(COO)\text{-}\nu_{sym}(COO)]$ between these frequencies for **2** is close to that found for anisobidentate (227 cm^{-1}) and bridging bidentate carboxylato groups (124 cm^{-1}), for **3** (250 cm^{-1}) is close to that observed for asymmetric bidentate chelate mode [4,5,12]. This is totally consistent with the X-ray structures. Two bands at 490–470 for **2**, are assigned to $\nu_{as,sym}(SnO)_2$, indicating non-linear O–Sn–O moieties, while the bands at 250–200 cm^{-1} are assigned to the tin–oxygen (COO) stretching modes [4,5,12].

3.2.2. NMR spectra

Table 5 gives the ^1H and ^{13}C-NMR chemical shifts of ligand and its complexes in $CDCl_3$ solution. The downfield chemical shift for HN in the spectra of ligand indicates that this proton is involved in hydrogen bonding. The existence of the HN resonance in the ^1H-NMR spectra of complexes indicates that the nitrogen atom remain protonated and the downfield chemical shift for this group indicates that this proton is involved in an intramolecular hydrogen bond between the HN group and the carbonyl oxygen of the carboxylato group. Deshielding of protons H(3) and H(4) is observed in complex **3**, which should be related to the electrophilicity of the tin. A σ-charge donation from the COO– donor to the tin center removes electron density from the ligand and produces this deshielding which will attenuate at positions remote from the metal. All shifts are downfield except for that due to H(5) which is shifted upfield. The upfield shift observed for H(5) and its corresponding carbon atom C(5), para to the tin center, could be due to the flow of charge from the tin into the aromatic ring [5,13]. Involvement of the carboxyl group in bonding to Sn is confirmed by the resonances ascribed to carboxyl carbon and C(3), which exhibit the greatest shifts upon coordination. The remaining resonances due to the aromatic carbon atoms do not shift significantly on binding to Sn. In the ^{13}C NMR spectra, the greatest downfield shift is exhibited by the C(2) (7.4 ppm) and the carbonyl C (7.0 ppm) for **3**. The C(5) resonance, by contrast, shifts upfield. Shielding of protons H(3), H(4) and H(6) is observed in complex **2**, which could be due to the flow of charge from the tin into the aromatic ring [5,13].

3.2.3. Electronic spectroscopy

The electronic spectrum of HDMPA in DMF solution exhibits two broad bands at ≈338 and 275 nm. The band at 338 nm is assigned to a $\pi \rightarrow \pi^*$ and the band at 275 nm is assigned to a $\pi \rightarrow \pi^*$ transition. The electronic spectra of the complexes are shown in Fig. 4. The complexes 2 and 3 were studied by the extended-Hückel

Table 5
^1H and ^{13}C-NMR data[a]

	COOH	NH	H(3)	H(4)	H(5)	H(6)	H(3′)-H(5′)	2′-CH_3, 6′-CH_3
HDMPA	[b]	8.90s	8.04d	6.66t	7.27t	6.22d	7.15	2.22s
2	Bu_2Sn: H_δ:0.82, H_γ:1.25, H_β:1.76, H_α,:1.40m	9.20s	7.91d	6.47d	7.36t	6.19d	7.13	2.198s
3	Bu_2Sn: H_δ:0903, H_γ:1.269, H_β:1.830, H_α:1.431m	8.92S	8.12d	6.69d	7.23t	6.21d	7.14	
	COOH	C(1)	C(2)	C(3)	C(4)	C(5)	C(6)	2′-CH_3 3′-CH_3
HDMPA	170.68	150.64	116.2	132.5	115.7	135.6	112.7	18.2
3[a]	COOH 177.6	156.8	126.1	133.3	115.6	134.8	110.4	18.3
	Bu_2Sn: C_γ:26.8 C_δ :13.5 C_α:25.6 C_β:26.3							

[a] Spectra recorded in $CDCl_3$.
[b] Carboxyl proton exchanged in $CDCl_3$.

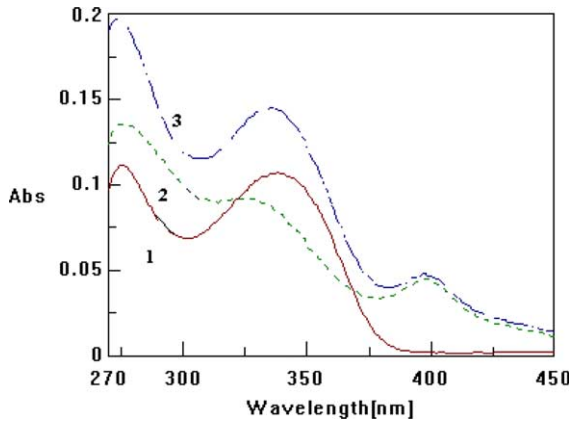

Fig. 4. Electronic absorption spectra of ligand **1** and diorganotin complexes **2** and **3** in DMF solution (5×10^{-5}).

method using the CACAO PC Beta-Version 5.0 package geometry [14]. The molecular geometry was established by using the crystallographic coordinates of the complexes 2 and 3. The extended-Hückel calculation using the crystallographic coordinates of **2** gives the following results: the HOMO orbital (−9.866 eV) is composed of p_x orbitals from Sn(1)p_x 14%(+), Sn(2)p_x 13%(+), of p_y from Sn(2)p_y 34%(−), O(2A)p_y 5%(−) and of p_z orbital from Sn(1) p_z 6%(−); the LUMO orbital (−9.309 eV) is composed of p_z orbitals from O(3)p_z 4%(+), O(4)p_z 5%(+), C(16)p_z 26%(−), C(18)p_z 10%(+), C(20)p_z 13%(−) and C(22)p_z 6%(+). The extended-Hückel calculation using the crystallographic coordinates of **3** gives the following results: the HOMO for (−11.476) eV) is composed of p_z orbitals from Sn(1) p_z 7%(−), C(17A)p_z 13%(+), C(16B)p_z 6%(+), C(17B)p_z 8%(−), C(18B)p_z 8%(+) and p_y orbitals from C(16B) p_y 15%(+); the LUMO (−9.316 eV) is composed of p_z from O(1A)p_z 5%(−), C(1A)p_z 28%(+), C(5A)p_z 11%(+), C(7A)p_z 11%(−) and p_y orbitals from C(1A) p_y 5%(+).

The broad band at 398 nm for **2** and **3** respectively is assignable to Homo–Lumo transition. The Homo orbital for **2** is mainly centered on metal centers Sn(1) and Sn(2) while the Lumo orbital is centered on an anthranilic ring. The Homo orbital for **3** is a mixed orbital centered on the metal Sn center and the donor carbon atoms while the Lumo orbital is centered on an anthranilic ring. The strong broad bands at 329 and 336 for **2** and **3** respectively are assignable to intraligand and charge transfer transitions [15], and the strong band at ≈275 and 273 nm for **2** and **3** is assigned to intraligand transition.

4. Supplementary material

Crystallographic data i.e., atomic coordinates, thermal parameters, bond lengths and bond angles) CCDC numbers 218732 and 218733 for **2** and **3** respectively, have been deposited with the Cambridge Crystallographic Data Centre as supplementary publication no. CCDC-1003/m. Copies of available material can be obtained, free of charge, on application to CCDC, 12 Union Road, Cambridge CB2 1EZ, UK, (fax: +44-1223-336033 or e-mail: deposit@ccdc.cam.ac.uk.

References

[1] (a) J.S. Kaltenbrom, R.A. Scherrer, F.W. Short, H.R. Beatty, M.M. Saka, C.V. Winder, J. Wax, W.R.N. Williamson, Arzneim.-Forsch./Drug Res. 33 (1) (1983) 621;
(b) D.K. Chalmers, G.H. Scholz, D.J. Topliss, E. Koliniatis, S.L.A. Munro, D.J. Craik, M. Iskander, J.R. Stockigt, J. Med. Chem. 36 (1993) 1272.

[2] A.G. Davies, Organotin Chemistry, VCH, Weinheim, 1997;
P.J. Smith (Ed.), Chemistry of Tin, second ed., Blackie Academic and Professional, London, England, 1998.

[3] (a) M. Gielen, Appl. Organomet. Chem. 16 (2002) 481;
(b) M. Gielen, Coord. Chem. Rev. 15 (1996) 41;
(c) S.J. Blunden, P.A. Cusack, R. Hill, Industrial Uses of Tin Chemicals, Royal Society of Chemistry, London, 1985;
(d) A.J. Crowe, in: M. Gielen (Ed.), Metal-Based Antitumour Drugs, vol. 1, Freund, London, 1989.

[4] (a) P. Tauridou, U. Russo, G. Valle, D. Kovala-Demertzi, J. Organomet. Chem. 44 (1993) C16;
(b) D. Kovala-Demertzi, P. Tauridou, A. Moukarika, J.M. Tsangaris, C.P. Raptopoulou, A. Terzis, J. Chem. Soc. Dalton (1995) 123;
(c) D. Kovala-Demertzi, P. Tauridou, U. Russo, M. Gielen, Inorg. Chim. Acta 239 (1995) 177;
(d) N. Kourkoumelis, A. Hatzidimitriou, D. Kovala-Demertzi, J. Organomet. Chem. 514 (1996) 163;
(e) S.K. Hadjikakou, M.A. Demertzis, J.R. Miller, D. Kovala-Demertzi, J. Chem. Soc. Dalton Trans (1999) 663.

[5] (a) V. Dokorou, Z. Ciunik, U. Russo, D. Kovala-Demertzi, J. Organomet. Chem. 630 (2001) 205;
(b) D. Kovala-Demertzi, N. Kourkoumelis, A. Koutsodimou, A. Moukarika, E. Horn, E.R.T. Tiekink, J. Organomet. Chem. 620 (2001) 194;
(c) N. Kourkoumelis, D. Kovala-Demertzi, E. Tiekink, Z. Crystallogr. 214 (1999) 758.

[6] (a) PATTY: P.T. Beurskens, G. Admiraal, G. Beurskens, W.P. Bosman, S. Garcia-Granda, R.O. Gould, J.M.M. Smits, C. Smykalla, 1992;
(b) SAPI91: Fan Hai-Fu. Structure Analysis Programs with Intelligent Control, Rigaku Corporation, Tokyo, Japan, 1991
(c) P.T. Beurskens, G. Admiraal, G. Beurskens, W.P. Bosman, R. de Gelder, R. Israel, J.M.M. Smits, The DIRDIF-94 program system, Technical Report of the Crystallography Laboratory, University of Nijmegen, 1994;
(d) G.M. Sheldrick, SHELXL97, program for crystal structure refinement, University of Göttingen, 1997.

[7] (a) D.T. Cromer, J.T. Waber, in: International Tables for X-ray Crystallography, vol. 4, The Kynoch Press, Birmingham, England, 1974, Table 2.2 A;
(b) J.A. Ibers, W.C. Hamilton, Acta Crystallogr. 17 (1964) 781;
(c) D.C. Creagh, W.J. McAuley, in: A.J.C. Wilson (Ed.), International Tables for Crystallography, vol. C, Kluwer Academic Publishers, Boston, 1992, Table 4.2.6.8;
(d) teXsan for Windows version 1.06: Crystal Structure Analysis Package, Molecular Structure Corporation, 1997;
(e) L.J. Farrugia, J. Appl. Cryst. 32 (1999) 837;
(f) A.L. Spek, PLATON.A Program for the automated generation of a variety of geometrical entities, University of Utrecht, The Netherlands, 2002.

[8] (a) K.C. Molloy, T.G. Purcell, K. Quill, I.W. Nowell, J. Organomet. Chem. (1984) 267;
(b) A.R. Forrester, S.J. Garden, R.A. Howie, J.L. Wardell, J. Chem. Soc. Dalton Trans. (1992) 2615.
[9] A. Addison, R.T. Nageswara, J. Reedijk, J. Van Rijn, G.C. Verschoor, J. Chem. Soc. Dalton Trans. (1984) 1349.
[10] V. Chandrasekhar, R.O. Day, J.M. Holmes, R.R. Holmes, Inorg. Chem. 27 (1988) 958.
[11] (a) E.R.T. Tiekink, Appl. Organomet. Chem. 5 (1991) 1;
(b) E.R.T. Tiekink, Trends Organomet. Chem. 1 (1994) 71.
[12] K. Nakamoto, Infrared and Raman Spectra of Inorganic and Coordination Compounds, fourth ed., Wiley, New York, 1986.
[13] M.A. Demertzis, S.K. Hadjikakou, D. Kovala-Demertzi, A. Koutsodimou, M. Kubicki, Helvet. Chim. Acta 83 (2000) 2787.
[14] (a) C. Mealli, D. Proserpio, CACAO PC Beta-Version 5., 1998;
(b) C. Mealli, D. Proserpio, J. Chem. Educ. 11 (1990) 440.
[15] (a) A. Galani, M.A. Demertzis, M. Kubicki, D. Kovala-Demertzi, Eur. J. Inorg. Chem. 9 (2003) 1761;
(b) P. Nath Yadav, M.A. Demertzis, D. Kovala-Demertzi, S. Skoulika, D.X. West, Inorg. Chim. Acta 349 (2003) 30;
(c) D. Kovala-Demertzi, N. Kourkoumelis, M.A. Demertzis, John R. Miller, C. Frampton, D.X. West, Eur. J. Inorg. Chem. (2000) 727.